

# The Speed and Position Sensorless Control of Switched Reluctance Motor using Binary Observer

Lee Woo Yang<sup>\*</sup>

Young Cho Kim<sup>\*</sup>

Jung Soo Choi

Young Seok Kim

Dept. of Electrical Engineering, Inha  
University

253 Yonghyun-dong, Nam-gu, Incheon, Korea  
Phone +82-32-860-7397 Fax+82-32-863-5822

<sup>°</sup> Dept. of Control & Instruments,  
Yuhan Junior College

185-34, Koean-dong, Puchon, Kyongki, Korea  
Phone +82-2-610-0831

## Abstract

It is well known that an encoder or a resolver is necessary to obtain the position data for speed or position control.

Generally utilized speed sensors are mal-affected by the EMI, dusty, and high temperature surroundings. Therefore, the speed and position sensorless controls using observers have been studied widely.

In this paper, the binary observer which is composed of two feedback regulation loops to control the speed of SRM(Switched Reluctance Motor) is applied. One loop compensates the control input directly like the sliding mode control, and the other one compensates the system parameters indirectly. This observer is constructed on the foundation of variable structure control theory and has the inertial term for the varying parameter. The validities of this proposed method is proved by experiments.

## 1. Introduction

The operational nature of SRM is determined by its specific structure. The stator and rotor

of SRM are all salient forms, the stator has concentrated windings which generate flux. These simple structure makes the SRM be small size, economical in price, and efficient in the sight of torque per unit cell in energy saving aspects.

The position sensors are not acceptable in the heavy electro magnetic environments, so the sensorless control methods have been studied during the past decades for motor(i.e. induction motor, permanent magnet motor and Reluctance motor). The SRM generates more electromagnetic noises than other motors in a wide range drives, and control with speed sensors decreases the system reliability.

Among the indirect position sensing methods, observer theories are widely applied because the observer is apt to get the real time compensation ability. But the conventional observers are acceptable merely in the linear system so, they showed the severe errors which come from the varying parameters and loads in the nonlinear system.

We overcome these faults effectively by using the binary observer. Specially, By adopting the inertial term in the estimation, the chattering problems shown in the system which has

discontinuous control inputs are reduced considerably. The rapid speed response and estimation performance for the load variation is obtained. PWM current control and angle control are used in this paper. In angle control, the firing-on and off angle determination is invited in this paper.

The proposed observer is implemented by DSP(Digital Signal Processor, TMS320C31) and gains are set by stability analysis.

## 2. The Structure of SRM

Fig1. shows the structure and drive system for one phase of SRM.

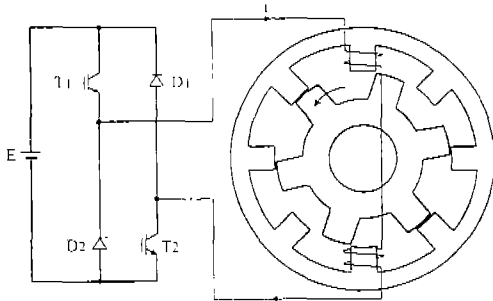


Fig1. The structure of 8/6 SRM

Rotor and stator are all salient pole form, and motor ratings are shown in Table 1.

Table 1. represents the SRM ratings which are used in the experiments.

Table 1. Motor Ratings

phases stator/rotor poles	8/6
Stator pole-arc	22.8[Deg]
Rotor pole-arc	24.6[Deg]
Phase resistance	1.6
Rated Torque	0.8[N.m]
Rated Speed	4000[rpm]
Dc-link Voltage	200[V]

Real inductance profiles versus position for one phase is shown in Fig2. The data in Fig2. are

obtained by braking test. These nonlinear inductance profiles are idealized to the linear inductance as Fig3. The maximum value of a phase inductance(Aligned) is 0.072 [H], and the minimum value (Unaligned) is 0.009[H].

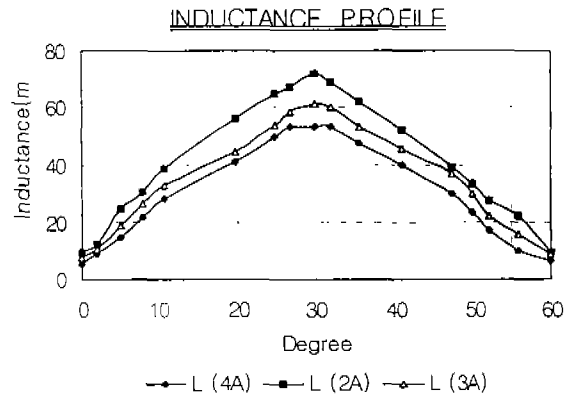


Fig2. Real Inductance Profile

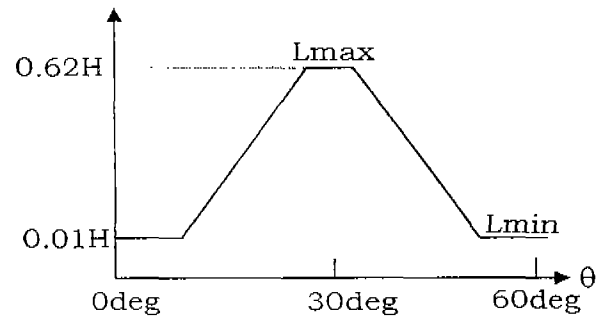


Fig3. Ideal Inductance Profile versus position

## 3. The Speed Control of SRM.

### 3.1 State Equation of SRM

The dynamic equations of SRM are shown below.

$$V = Ri + L(\theta, i) \frac{di}{dt} + \frac{dL(\theta, i)}{d\theta} \omega i \quad (1)$$

$$T(\theta, i) = J \frac{d\omega}{dt} + B\omega + T_L$$

$$= \frac{1}{2} i^2 \frac{dL(\theta, i)}{d\theta}$$

In the (1),  $V$  is a applied voltage in the one phase. The state equation are acquired as (2)

$$\begin{aligned} \frac{d}{dt} i &= -\frac{R}{L} i - \frac{dL}{L d\theta} \omega i + \frac{V}{J} \\ \frac{d}{dt} \omega &= -\frac{B}{J} \omega + \frac{T - T_L}{J} \\ &= \frac{1}{2J} i^2 \frac{dL}{d\theta} - \frac{T_L}{J} - \frac{B}{J} \omega \end{aligned} \quad (2)$$

where,

$$\begin{aligned} i &= [i_a \ i_b \ i_c \ i_d]^T \\ L &= [L_a \ L_b \ L_c \ L_d]^T \end{aligned}$$

### 3.2 Control of Current and Angle

The current is controlled between two current levels equals to  $i_{ref} \pm \frac{\Delta i}{2}$  where,  $i_{ref}$  = reference current, and  $\Delta$  = hysteresis band. The real current follows the reference current as shown in Fig4.

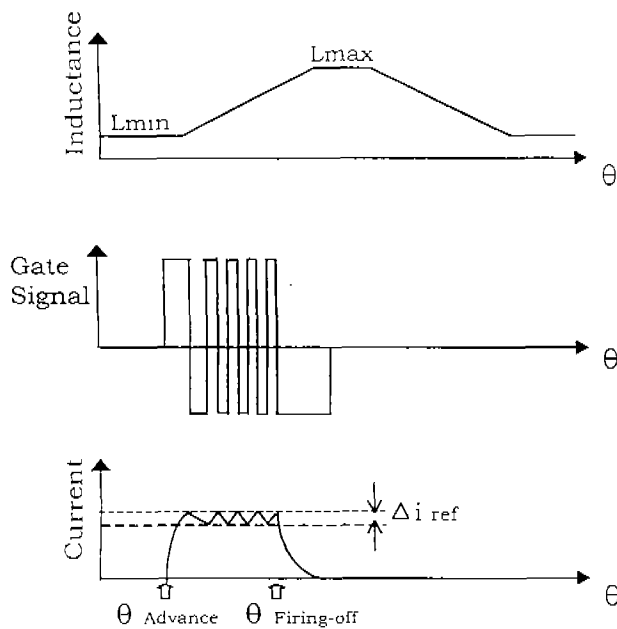


Fig4. PWM Current Control

It is desirable to apply a square current waveform during the conduction period of a phase. However, this is not practical since the motor phase has a considerable amounts of inductance and it takes times for the current to rise and fall. As the back

EMF increases, it reduces the effective voltage applying to the phase and increases the rising time for the current to reach the commanded level. Therefore, the effect of back EMF should be considered to determine the turn-on and turn-off time for excitation of SRM.

Turn-on point of one phase should be earlier on than meeting point to the rising slope of the inductance. Similarly, the firing-off angle should have the enough margin for the current tail not to touch the negative torque region.

### 4. Current and Speed Observer

Generally the state observer theory is adopted in the linear system, but SRM has an nonlinear equations. So the non-linearity of states are pre-assumed as following conditions.

First, during the one sampling time, speed and inductance perturbations could be neglected.

Second, the inductance rising or falling slope is constant. As for this assumptions, the observer equation is as the (3).

$$\begin{aligned} \frac{d}{dt} i_e &= -\frac{R}{L_e} i_e - \frac{dL_e}{L_e d\theta_e} \omega_e i_e + \frac{V}{J} + K_1 \nu \\ \frac{d}{dt} \omega_e &= -\frac{B}{J} \omega_e + \frac{T_e - T_L}{J} \\ &= \frac{1}{2J} i_e^2 \frac{dL_e}{d\theta_e} - \frac{T_L}{J} - \frac{B}{J} \omega_e + K_2 \nu \end{aligned} \quad (3)$$

where,

$$\begin{aligned} i_e &= [i_{ae} \ i_{be} \ i_{ce} \ i_{de}]^T \\ L_e &= [L_{ae} \ L_{be} \ L_{ce} \ L_{de}]^T \end{aligned}$$

$$K_1 = k_1 I, \quad K_2 = k_2 I_1$$

$$\nu I = [\mu I \ \sigma_i]$$

$$I: [4 \times 4] \text{ Identity matrix}$$

$$I_1: [1 \ 1 \ 1 \ 1]$$

$$\dot{\mu} = -\alpha \cdot [\mu(t) - \text{sgn}(\sigma(t))]$$

$$\begin{aligned} \sigma &= [(i_a - i_{ae})(i_b - i_{be}) \\ &\quad (i_c - i_{ce})(i_d - i_{de})]^T \end{aligned}$$

#### 4.1 Gain setting and Error equation

Equation(4), Fig5 shows the boundary region and the error trajectory of the binary observer.

$$\begin{aligned} G_\delta &= x : \sigma^+ \cdot \sigma^- \leq 0 \\ \sigma^- &= \sigma - \delta \quad \delta : \text{const} \\ \sigma^+ &= \sigma + \delta \quad 0 \leq \delta \leq 1 \end{aligned} \quad (4)$$

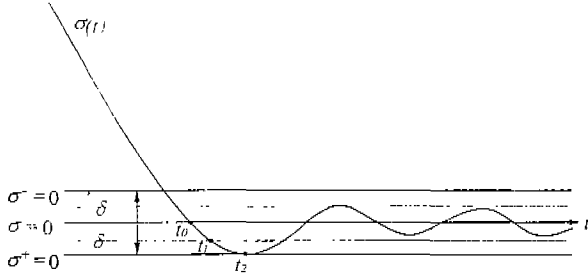


Fig5. Boundary region and the error trajectory

The error equation is obtained by (2) - (3) and then, linearize the result as followings.

$$\frac{d}{dt} \begin{bmatrix} e_i \\ e_\omega \end{bmatrix} = \begin{bmatrix} F_{11} & F_{12} \\ F_{21} & F_{22} \end{bmatrix} \begin{bmatrix} e_i \\ e_\omega \end{bmatrix} + \begin{bmatrix} K_1 \\ K_2 \end{bmatrix} \nu \quad (5)$$

where,  $e_i = i_e - i$ ,  $e_\omega = \omega_e - \omega$

$$F_{11} = \left[ -\frac{R}{L} - \frac{1}{L} \frac{dL}{d\theta_e} \omega_e \right] I,$$

$$F_{12} = \left[ -\frac{1}{L} \frac{dL}{d\theta_e} i \right] I_1^T$$

$$F_{21} = \frac{1}{J} \left[ \frac{1}{L} \frac{dL}{d\theta_e} i \right] I_1, \quad F_{22} = \frac{-B}{J}$$

To converge the estimation errors to 'zero' the (6) should be satisfied.

$$\sigma^+(t) \cdot \dot{\sigma}^+(t) < 0, \quad \sigma^-(t) \cdot \dot{\sigma}^-(t) < 0 \quad (6)$$

And, to have the inertia character of the binary observer the  $\mu$  in the (7) should be satisfied.

$$\begin{aligned} -\mu(t_2) \operatorname{sgn} \sigma(t) &\geq 1 - h \\ \text{where, } 0 < h < 1 \end{aligned} \quad (7)$$

##### 1) Primary-loop Gain

From the (5) and the (7),  $K_1$  could be obtained in each case of  $\sigma > 0$  and  $\sigma < 0$ .

$$K_1 > \max \left\{ \begin{aligned} & \sup \left| \frac{1}{(-1+h)\delta} [F_{11}\delta + F_{12}e_\omega] \right| \\ & , \sup \left| \frac{1}{(1-h)\delta} [F_{11}\delta - F_{12}e_\omega] \right| \end{aligned} \right\} \quad (8)$$

From the (5), when the error come in the  $G_\delta$  region the condition that converges the error to 'zero' is acquired by setting the first term in the (5) as a constant value.

$$\begin{aligned} \dot{e}_i &= d = F_{11}e_i + F_{12}e_\omega + K_1\nu \\ \text{where, } d &: \text{const} \end{aligned} \quad (9)$$

And, the (10) is acquired by substituting the second term in the (5) by the (9).

$$\begin{aligned} \dot{e}_\omega &= (F_{21} - K_2K_1^{-1}F_{11})\delta + (F_{22} \\ & - K_2K_1^{-1}F_{12})e_\omega + K_2K_1^{-1}d \end{aligned} \quad (10)$$

Therefore, the  $e_\omega$  could be converged to 'zero' by setting the eigen value of the  $F_{22} - K_2K_1^{-1}F_{12}$  term in the (10) as a negative value, which is shown at the (11).

$$K_2 < \frac{B}{J} L_e \frac{d\theta_e}{dL_e} \frac{1}{i_e} K_1 \quad (11)$$

##### 2) Secondary loop Gain

The Gain  $\alpha$  could be obtained by contradicting the inequality in the (7). And the result is the (12).

$$\alpha > \frac{1}{\delta} \bar{K} \cdot \ln \frac{2}{h} \quad (12)$$

where,  $\bar{K} = \sup |F_{11}e_i + F_{12}e_\omega + K_1\nu|$

We coincided the estimation states with the real system states by using the gain obtained from the inequalities (8) and (12). As a results, we acquired the good estimation performance.

### 4.2 Binary observer System

The binary observer has the two feedback updating loops as shown in Fig.5.

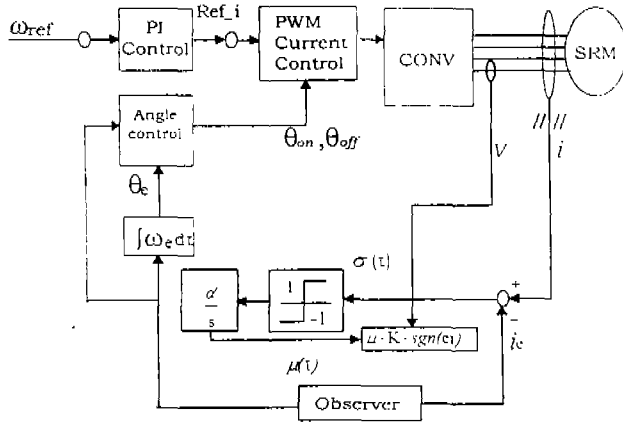


Fig5. Binary block diagram

## 5. Experimental Results

The total block diagram is showed in Fig.6.

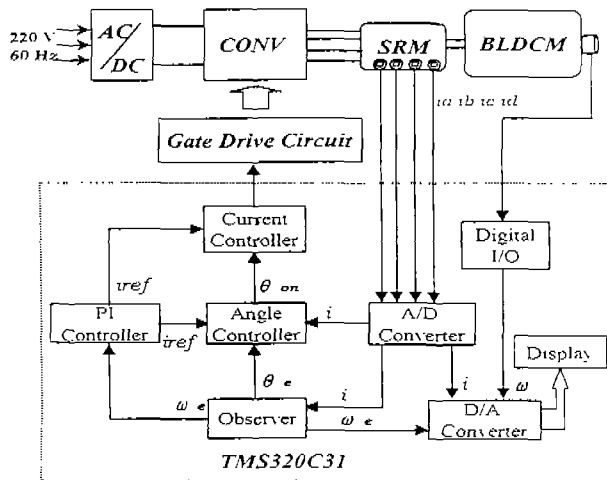
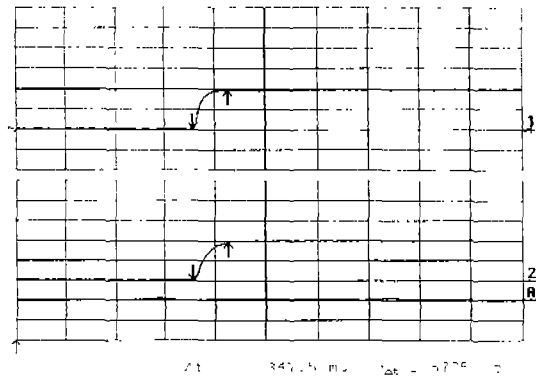


Fig6. The total system block diagram

The blocked part implemented by DSP(Digital Signal Processor. TMS320C31 )operates the current estimation, the speed identification and position estimation, PWM current control, and the calculation of advance and Firing-off angle. The applied converter is a asymmetrical type and

Next, the experiment results are shown in the

0.4N.m load. In Fig7. the real speed(Ch1), estimated speed(Ch2), and their error(ChA) are presented when the 1000rpm is commanded by speed reference.



Ch1 500rpm/div Ch2 500rpm/div ChA 250rpm/div 0.5sec/div

Fig7. Experiment result of Speed

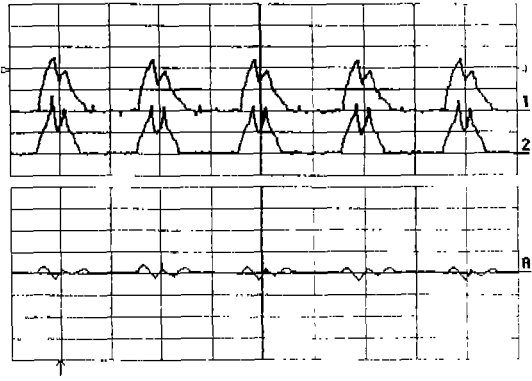
This observer estimates the speed with little error, and reach the reference value within 0.345sec without overshoot.

There is little chattering in the speed which is often appeared in the sliding mode control. because the continuous control input terms in the proposed observer prevents the chattering.

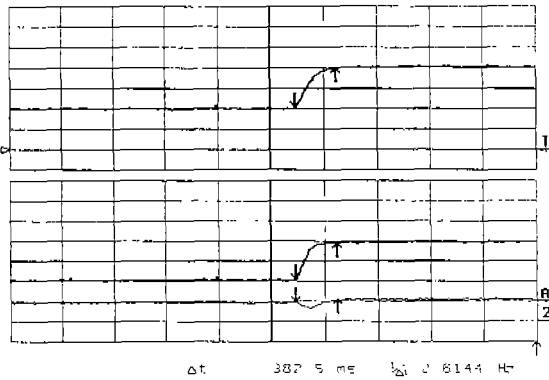
Fig8. Shows the real current(Ch1), estimated current(Ch2), and estimation error(ChA).

Current is controlled by PWM rule near the 4[A] level. The real current is estimated stably with a little error.

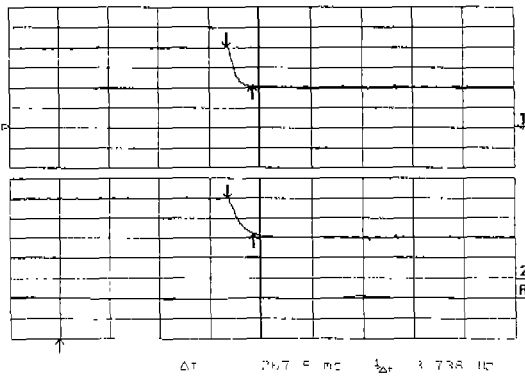
Fig9. and Fig10. presents the real speed(Ch1), estimated speed(Ch2), and their error(ChA) when the accelerating and the decelerating speed reference is commanded. In each case this observer shows the good speed estimation performance and good reference pursuing ability with a small transient errors. And the speed error converges to '0' quickly in each case. Even the large inertia load, robust parameter estimation performance is retained.



Ch1 2[A] div Ch2 2[A] div ChA 2[A] div 2[ms] div  
 Fig8. Experiment result of one phase current



Ch1 500rpm/div Ch2 500rpm/div ChA 250rpm/div 0.5sec/div  
 Fig9. Speed in the acceleration command



Ch1 500rpm/div Ch2 500rpm/div ChA 250rpm/div 0.5sec/div  
 Fig10. Speed in the deceleration command

## 6. Conclusion

This newly proposed observer system is established on the basis of the estimated currents and torque

using the linearly approximated inductance.

The estimation performance of this proposed observer verified in the experiment results. Specially, the additive inertia terms in observer reduced the chattering phenomenon considerably as shown in the test results.

## Reference

- [1] S. K. Panda, and G. Amaratunga, "Switched Reluctance Motor Drive Without Direct Rotor Position Sensing", IEEE IAS Annual Meeting, pp.525-530, 1990.
  - [2] A. Lumsdaine, J. H. Lang, "State Observer for Variable-Reluctance Motor", IEEE Trans. IE, Vol. IE-37, No.2, pp.133-142, 1990.
  - [3] C.Elmas, H.Z.L. Parra, "Position Sensorless Operation of a Switched Reluctance Drive Based on Observer". EPE, pp.82-87, 1993.
  - [4] S.Kim, J.Kim, H.Kim, Y. Kim, "Binary Observer for Speed Sensorless Vector Control of Induction Motor", IEEE PESC, Vol.2, pp.1061-1067, 1997.
  - [5] S.V.Emelyanov, "Binary Automatic Control" System. Mir Publisher Moscow, 1987.
- Operation of a Switched Reluctance Drive Based on Observer", EPE, pp.82-87, 1993.